Functions of vasopressin and oxytocin in bone mass regulation

Li Sun[a,1], Roberto Tamma[b,1], Tony Yuen[a,1], Graziana Colaianni[b], Yaoting Ji[a], Concetta Cuscito[b], Jack Bailey[a], Samarth Dhawan[a], Ping Lu[a], Cosima D. Calvano[c], Ling-Ling Zhu[a], Carlo G. Zambonin[c], Adriana Di Benedetto[d], Agnes Stachnik[a], Peng Liu[a], Maria Grano[b], Silvia Colucci[b], Terry F. Davies[a], Maria I. New[a,2], Alberta Zallone[b,3], and Mone Zaidi[a,2,3]

[a]The Mount Sinai Bone Program, Department of Medicine, Icahn School of Medicine at Mount Sinai, New York, NY 10029; [b]Department of Basic Medical Science, Neurosciences and Sensory Organs, University of Bari, 70124 Bari, Italy; [c]Department of Chemistry, University of Bari Aldo Moro, Bari 70124, Italy; and [d]Department of Clinical and Experimental Medicine, University of Foggia, Foggia 71122, Italy

Contributed by Maria I. New, December 1, 2015 (sent for review September 10, 2015; reviewed by Xu Cao, Ernestina Schipani, and Rajesh V. Thakker)

Prior studies show that oxytocin (Oxt) and vasopressin (Avp) have opposing actions on the skeleton exerted through high-affinity G protein-coupled receptors. We explored whether Avp and Oxtr can share their receptors in the regulation of bone formation by osteoblasts. We show that the Avp receptor 1α (Avpr1α) and the Oxt receptor (Oxtr) have opposing effects on bone mass: *Oxtr*$^{-/-}$ mice have osteopenia, and *Avpr1α*$^{-/-}$ mice display a high bone mass phenotype. More notably, this high bone mass phenotype is reversed by the deletion of *Oxtr* in *Oxtr*$^{-/-}$:*Avpr1α*$^{-/-}$ double-mutant mice. However, although Oxtr is not indispensable for Avp action in inhibiting osteoblastogenesis and gene expression, Avp-stimulated gene expression is inhibited when the Oxtr is deleted in *Avpr1α*$^{-/-}$ cells. In contrast, Oxt does not interact with Avprs in vivo in a model of lactation-induced bone loss in which Oxt levels are high. Immunofluorescence microscopy of isolated nucleoplasts and Western blotting and MALDI-TOF of nuclear extracts show that Avp triggers Avpr1α localization to the nucleus. Finally, a specific Avpr2 inhibitor, tolvaptan, does not affect bone formation or bone mass, suggesting that Avpr2, which primarily functions in the kidney, does not have a significant role in bone remodeling.

osteoporosis | osteoblast | skeleton

Over the past decade, we have described direct actions of anterior and posterior pituitary hormones on the skeleton (1–8). We have shown that these actions are exerted via G protein-coupled receptors resident on both osteoblasts and osteoclasts. We also find that the skeleton is highly sensitive to the action of posterior pituitary hormones; for example, mice haploinsufficient in oxytocin (Oxt) have osteopenic bones, but lactation is normal; lactation is impaired only in *Oxt*$^{-/-}$ mice (2). Likewise, *Tshr* haploinsufficient mice are completely euthyroid with normal thyroid follicles but display significant osteopenia (4). The exquisite sensitivity of the skeleton to pituitary hormones comes as no surprise, considering that the pituitary gland and the skeleton are both evolutionarily more primitive than target endocrine organs (7).

Apart from the known actions of growth hormone on the skeleton, Tsh, Fsh, Acth, Oxt, and vasopressin (Avp) have all been shown to regulate the formation and/or function of both osteoblasts and osteoclasts and thus to control bone remodeling in vivo (2–4, 6–8). The two neurohypophyseal hormones Oxt and Avp have opposing functions (2, 3). Oxt stimulates and Avp inhibits osteoblast formation. Consequently, the genetic deletion of the Oxt receptor (Oxtr) and Avp receptor 1α (Avpr1α) yields opposing phenotypes, notably osteopenia in *Oxtr*$^{-/-}$ mice and high bone mass in *Avpr1α*$^{-/-}$ mice (2, 3). These findings may explain the rapid recovery of bone loss at weaning when plasma Oxt levels are high (9) and also the profound loss of bone noted in chronic hyponatremic states, such as the syndrome of inappropriate antidiuretic hormone secretion (SIADH), in which serum Avp levels are elevated (3).

We find high levels of Oxtr expression on both osteoclasts and osteoblasts (2, 10), in addition to their abundant expression in breast and uterine tissue, where they regulate lactation and parturition, respectively (11). Avpr1αs, in contrast, are distributed more ubiquitously, whereas Avpr2s are localized mainly in the kidney, where they regulate free water excretion (12). Osteoblasts express both Avpr1α and Avrpr2 (3). The only other known isoform, Avpr1β, is expressed predominantly in the pancreas and pituitary; it regulates ACTH secretion from pituitary corticotrophs (13). Sequence alignment shows that the binding sites of the Oxtr and Avprs are highly conserved, with specific amino acids within the predicted binding pocket providing ligand selectivity (14–16). The respective ligands Oxt and Avp also are homologous nonapeptides, differing in only two amino acids, and are known to interact with the other's receptor with different affinities (17).

To our knowledge, osteoblasts and osteoclasts are the only cells in which Oxtr, Avpr1α, and Avpr2 are coexpressed. We also have shown that osteoblastic Oxtrs undergo internalization and nuclear translocation upon binding to Oxt and that this action is independent of cytosolic Erk phosphorylation (18). Avpr1α activation by Avp also activates Erk phosphorylation within minutes (3). The homology between the ligands and their respective receptors and converging downstream signals suggest that Avp and Oxtr may share receptors with opposing or convergent signals. Here, we have explored these interactions in the regulation of osteoblastic bone formation by using mice lacking one or both receptors, chemical inhibitors, and physiological models of high bone turnover.

Significance

We show that oxytocin and vasopressin, which are released from the posterior pituitary gland to regulate lactation and water balance, respectively, are potent regulators of skeletal integrity. Using genetically modified mice and chemical inhibitors, we provide evidence that the two hormones interact with each other's receptors to control precisely the formation of new bone.

Author contributions: M.G., M.I.N., A.Z., and M.Z. designed research; L.S., R.T., T.Y., G.C., Y.J., C.C., J.B., S.D., P. Lu, C.D.C., L.-L.Z., C.G.Z., A.D.B., and A.S. performed research; L.S., R.T., T.Y., G.C., C.C., C.D.C., C.G.Z., P. Liu, S.C., T.F.D., M.I.N., A.Z., and M.Z. analyzed data; and L.S., T.Y., A.Z., and M.Z. wrote the paper.

Reviewers: X.C., Johns Hopkins School of Medicine; E.S., University of Michigan; and R.V.T., Academic Endocrine Unit, University of Oxford.

The authors declare no conflict of interest.

[1]L.S., R.T., and T.Y. contributed equally to this work.

[2]To whom correspondence may be addressed. Email: maria.new@mssm.edu or mone.zaidi@mssm.edu.

[3]A.Z. and M.Z. contributed equally to this work.

This article contains supporting information online at www.pnas.org/lookup/suppl/doi:10.1073/pnas.1523762113/-/DCSupplemental.

Results

Oxtrs and the three Avpr isoforms, namely Avpr1α, Avpr1β, and Avpr2, constitute a subfamily of G protein-coupled receptors, and their respective ligands, Avp and Oxt, are cyclic nonapeptides that closely resemble each other. Therefore we first assessed whether the ligands could cross-react with the Oxtr and Avpr receptors in the context of their opposing actions on the osteoblast. Consistent with its function, Avp strongly inhibited osteoblast formation in primary bone marrow stromal cell cultures from $Oxtr^{+/+}$ mice at both 1 and 2 wk (Fig. 1*A*). This inhibitory action was retained in osteoblast cultures derived from $Oxtr^{-/-}$ mice (Fig. 1*A*). Consistent with this result, at both time points Avp strongly attenuated the expression of most osteoblastic genes, namely, alkaline phosphatase (*Alp*), runt-related transcription factor 2 (*Runx2*), and activating transcription factor 4 (*Atf4*), but not *osterix* (Sp7 transcription factor 7, *Sp7*) (Fig. 1*B*). Taken together, these data suggest that the Oxtr is not indispensable for the antiosteoblastic action of Avp.

We sought to determine directly the extent of contribution of the Avpr and Oxtr to the Avp response. Quantitative PCR (qPPCR) showed that Avp triggered an early suppression of the expression of the osteoblast differentiation genes *osteocalcin* (bone γ-carboxyglutamic acid–containing protein, *Bglap*), *bone sialoprotein* (integrin-binding sialoprotein, *Ibsp*), *Runx2*, and *Sp7* in bone marrow stromal cell cultures from wild-type mice (Fig. 1*C*). This response was almost completely abrogated in $Avpr1\alpha^{-/-}$ cultures (Fig. 1*C*), establishing that Avpr1α is necessary for the inhibitory action of Avp. The reversal was less marked in cultures from double-mutant mice in which both *Avpr1α* and *Oxtr* were deleted (Fig. 1*C*). This finding suggested that Avp does, to some extent, interact with the Oxtr to exert a pro-osteoblastic action in $Avpr1\alpha^{-/-}$ cells. These interactions were confirmed at the protein

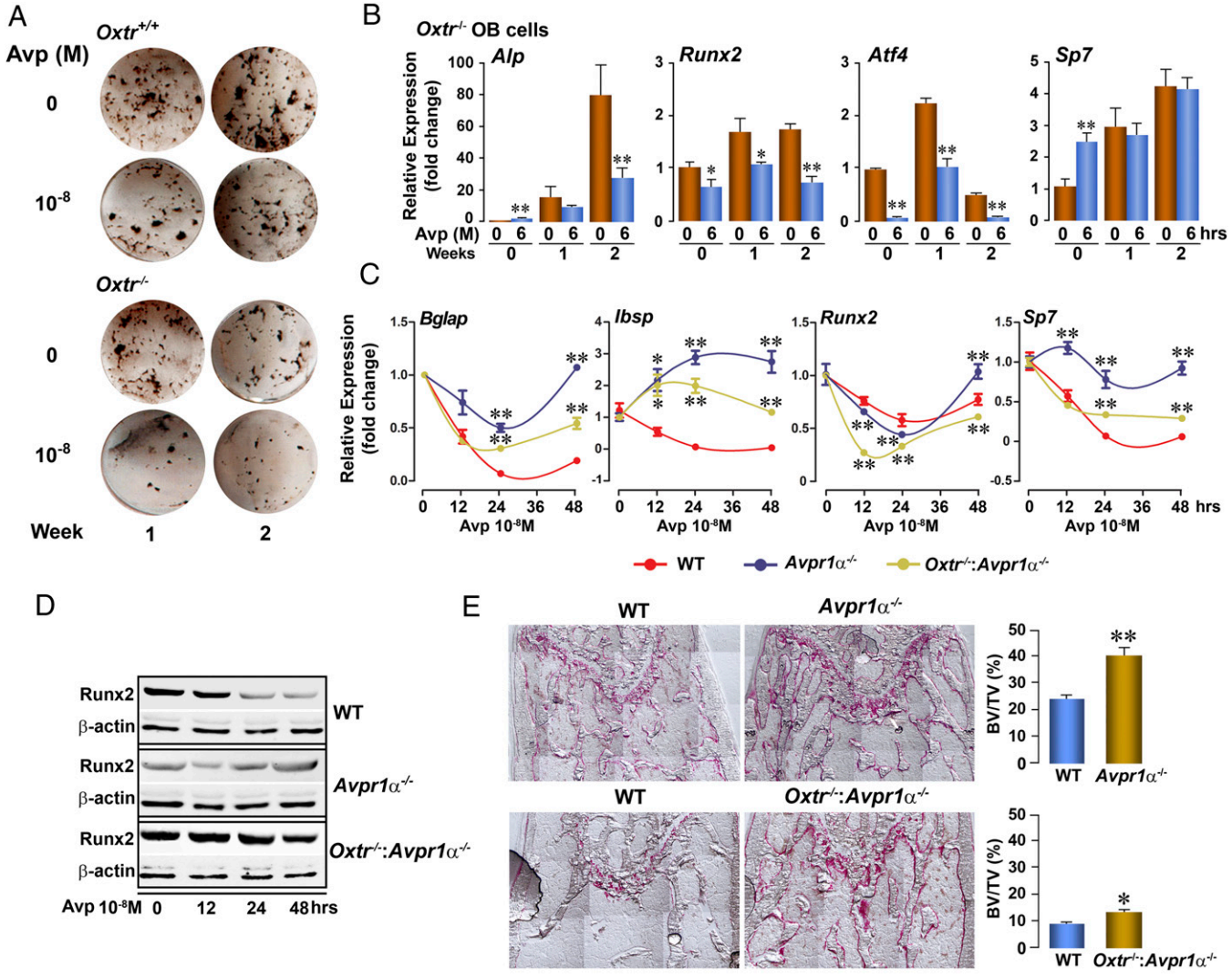

Fig. 1. Avp interacts with both osteoblast Avpr1α and Oxtr in bone mass regulation. (*A*) Representative wells showing the effect of Avp (10^{-8} M) on alkaline phosphatase-positive colonies 1 or 2 wk after the induction of differentiation in bone marrow stromal cell cultures isolated from $Oxtr^{-/-}$ or $Oxtr^{+/+}$ mice. (*B*) mRNA expression (by qPCR) of osteoblast genes, namely *Alp*, *Runx2*, *Atf4*, and *osterix* (*Sp7*), in differentiating bone marrow stromal cell cultures from $Oxtr^{-/-}$ mice following a 6-h exposure to Avp. $^*P < 0.05$, $^{**}P < 0.01$, triplicate. (*C* and *D*) Effect of Avp on mRNA expression (qPCR) of the osteoblast genes *osteocalcin* (*Bglap*), *bone sialoprotein* (*Ibsp*), *Runx2*, and *Sp7* (comparison with wild type at each time point, $^*P < 0.05$, $^{**}P < 0.01$, triplicate) (*C*) or Runx2 protein expression (Western blot) (*D*) in differentiating (10 d) bone marrow stromal cell cultures isolated from $Avpr1\alpha^{-/-}$, $Oxtr^{-/-}$:$Avpr1\alpha^{-/-}$, or wild-type mice. (*E*) Histomorphometry of spinal trabecular bone from $Avpr1\alpha^{-/-}$, $Oxtr^{-/-}$:$Avpr1\alpha^{-/-}$, or wild-type mice, expressed as fractional bone volume (BV/TV), together with representative images. $^*P < 0.05$, $^{**}P < 0.01$ compared with respective wild-type littermates, as shown. Results are shown as mean ± SEM. Statistics by unpaired Student's *t*-test, comparison with 0-dose control. $n = 5$ mice per group.

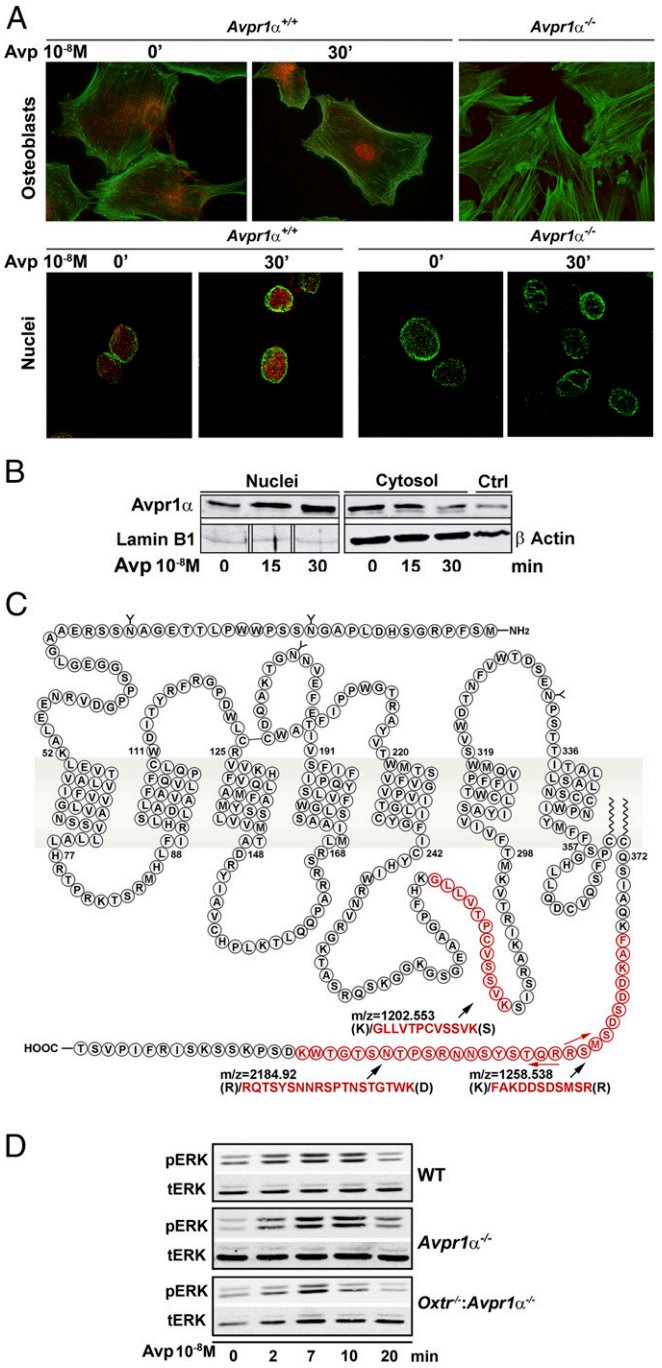

Fig. 2. Avp triggers nuclear localization of the Avpr1α. (*A*) Primary bone marrow stromal cells from *Avpr1α*$^{+/+}$ or *Avpr1α*$^{-/-}$ mice were stimulated with Avp (10^{-8} M, 30 min) and stained with anti-Avpr1α antibody (red). Green indicates phalloidin staining. (*Top*) Midsectional confocal microscopy shows that at 30 min there is complete nuclear localization of the Avpr1α in *Avpr1α*$^{+/+}$ cells, but this localization is absent in *Avpr1α*$^{-/-}$ cells. (*Lower*) The outer nuclear membrane was removed from isolated nuclei to produce nucleoplasts (19). Nuclei were stained with anti-Avpr1α antibody (red) and counterstained with anti-Kpnb1 antibody (green). Avpr1αs were visualized intranuclearly (red) at 30 min after Avp stimulation. *Avpr1α*$^{-/-}$ cells expectedly showed no staining with the Avpr1α antibody. (*B*) Primary osteoblasts were treated with Avp (10^{-8} M) for 15 or 30 min. Western blots show Avpr1α in the cytosolic and nuclear fractions. Markers included β-actin (cytosol) and lamin B1 (nuclear). Control (Ctl): whole-cell lysates. (*C*) Proteins in the immunoprecipitate from MC3T3.E1 preosteoblasts (with anti-Avpr1α antibody) were identified using MS-Fit software (prospector.ucsf.edu/prospector/cgi-bin/msform.cgi?form=msfitstandard), and all other proteins were recognized as nuclear proteins. Analysis of the spectra (FindPept database) revealed three peptides corresponding to Avpr1α intracellular loops in the in-gel band (45 kDa) at mass-to-charge ratios (*m/z*) of 1202.55 [(K)/GLLVTPCVSSVK/(S), residues 274–285], 1258.54 [(K)/FAKDDSDSMSR/(R), residues 378–388], and 2184.92 [(R)/RQTSYSNNRSPTNSTGTWK/(D), residues 389–407]. (*D*) Western immunoblot showing the effect of Avp (10^{-8} M) on the phosphorylation of Erk (pErk) in whole-cell lysates from bone marrow stromal cell cultures obtained from *Avpr1α*$^{-/-}$ or *Oxtr*$^{-/-}$:*Avpr1α* $^{-/-}$ or wild-type mice. Total Erk (tErk) is shown.

level: Avp inhibited *Runx2* expression at both 24 and 48 h in wild-type cells but did not do so in *Avpr1α*$^{-/-}$ cells (Fig. 1*D*). The extent of inhibition was less pronounced but not abrogated in *Avpr1a*$^{-/-}$:*Oxtr*$^{-/-}$ cells (Fig. 1*D*).

With knowledge from our previous studies that *Avpr1α*$^{-/-}$ mice display a high bone mass phenotype, notably with increases in osteoblast surface (Ob.S/BS) and fractional bone volume (BV/TV), we examined whether deleting *Oxtr* modifies this phenotype. Histomorphometry revealed an approximately threefold increase in BV/TV in *Avpr1α*$^{-/-}$ mice compared with wild-type littermates (Fig. 1*E*). However, BV/TV was not increased to the same extent (~25%) in the double-mutant *Avpr1α*$^{-/-}$:*Oxtr*$^{-/-}$ mice, compared with the respective wild-type littermates (Fig. 1*E*). Overall, the data show rescue of the *Avpr1α*$^{-/-}$ phenotype by Oxtr deletion, suggesting that Avpr1αs and Oxtrs have opposing effects in regulating bone mass.

Previously we have shown that exposure of osteoblasts to Oxt causes the transcytosolic movement and nuclear localization of the Oxtr (18). During this process, the Oxtr interacts with β-arrestin, Rab5, importin-β, and transportin-1 (18). Here, using immunostaining, Western immunoblotting, and MALDI-TOF, we show that Avp triggers the nuclear localization of Avpr1α in osteoblasts. Notably, immunofluorescence microscopy demonstrated that, under basal unstimulated conditions, Avpr1αs appear mainly at the plasma membrane and in the cytoplasm, whereas a clear nuclear localization was noted ~30 min after the addition of Avp (10^{-8} M) (Fig. 2*A*). To exclude potential artifacts arising from the extreme flatness of cultured cells or possible localization of Avpr1αs to membrane structures close to the nuclear compartment, we isolated intact nucleoplasts from primary murine osteoblasts. This method removes the outer nuclear membrane, providing pure fractions of nucleoplasts surrounded by the inner but not the outer nuclear membrane (19). Nucleoplasts were isolated after stimulation of intact osteoblasts with Avp (30 min) and were stained for Avp and importin-β (Kpnb1), a known inner nuclear membrane and nucleoplasm marker. Confocal microscopy revealed that, although there was minimal nuclear localization of Avpr1αs in unstimulated nucleoplasts, intense immunofluorescence was noted within the inner nuclear membrane upon Avp stimulation (Fig. 2*A*, *Center*). This localization was absent upon the stimulation of *Avpr1α*$^{-/-}$ cells, establishing specificity (Fig. 2*A*, *Right*).

Western immunoblotting was used further to study the presence of Avpr1αs in the cytosol and nuclear compartments of osteoblasts exposed to Avp for 15 or 30 min. At both time points, Avpr1αs were localized to the nuclear fraction with correspondingly reduced cytosolic protein at 30 min (Fig. 2*B*). Of note, unlike Oxtrs, Avpr1αs were localized to the nucleus even in untreated cells, as evident both on confocal microscopy and Western immunoblotting (Fig. 2 *A* and *B*). LaminB1, a nuclear membrane marker, and actin were unchanged upon Avp stimulation (Fig. 2*B*).

In separate experiments, nuclear proteins from MC3T3.E1 preosteoblasts were immunoprecipitated with anti-Avpr1α antibody and subject to MALDI-TOF analysis. Separation by SDS/PAGE was followed by in-gel digestion using trypsin and RapiGest SF (Waters) (18). This approach allowed almost all

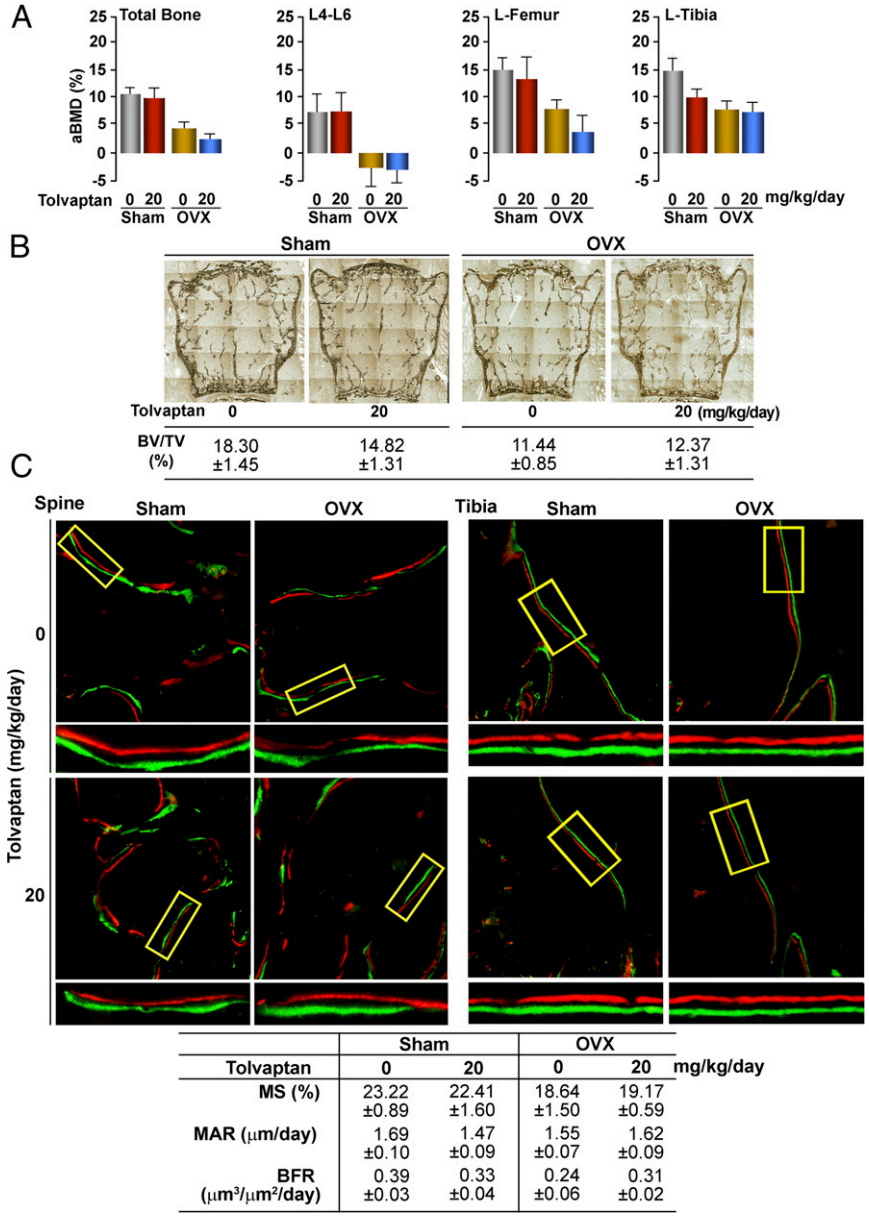

Tolvaptan	Sham 0	Sham 20	OVX 0	OVX 20	mg/kg/day
MS (%)	23.22 ±0.89	22.41 ±1.60	18.64 ±1.50	19.17 ±0.59	
MAR (μm/day)	1.69 ±0.10	1.47 ±0.09	1.55 ±0.07	1.62 ±0.09	
BFR (μm³/μm²/day)	0.39 ±0.03	0.33 ±0.04	0.24 ±0.06	0.31 ±0.02	

Fig. 3. Avpr2 inhibition does not affect bone formation or bone mass. (*A*) Effect of a specific Avpr2 inhibitor, tolvaptan (20 mg·kg^{-1}·d^{-1}), administered i.p. for 4 wk to sham-operated (Sham) or ovariectomized (OVX) mice, on BMD (PIXImus, Lunar-GE), expressed as total bone, spine (L4–L6), left femur (L-Femur), and left tibia (L-Tibia) BMD. (*B*) Fractional bone volume (BV/TV) assessed from von Kossa-stained sections of spinal trabecular bone (representative images are shown). (*C*, *Lower*) Bone formation parameters, namely mineralizing surface (MS), mineral apposition rate (MAR), and bone formation rate (BFR) following dual calcein (green) and xylenol orange (red) labeling. (*Upper*) Representative images are shown. Statistics: unpaired Student's *t* test, corrected for multiple comparisons by Bonferroni; vehicle versus tolvaptan in Sham and OVXgroups yielded $P > 0.1$; $n = 5$ mice per group.

proteins in the immunoprecipitate to be identified (using MS-Fit software); all other proteins were recognized as nuclear proteins. Analysis of spectra (FindPept database) in the excised band revealed the presence of three peptides corresponding to the Avpr1α intracellular loops (Fig. 2*C*), confirming that, after Avp activation, Avpr1αs move from the plasma membrane to the nucleus.

Because both Avp and Oxt signal through Erk, we asked whether Avp could signal through Erk phosphorylation in the absence of the Avp1α and, importantly, whether there was a residual pErk signal when both the Avpr1α and Oxtr were deleted. Indeed, Avp triggered Erk phosphorylation in wild-type, *Avpr1α*$^{-/-}$, and *Avpr1α*$^{-/-}$*:Oxtr*$^{-/-}$ cells (Fig. 2*D*). This finding suggested that a third receptor, Avpr2, was mediating the residual increase in pErk triggered by Avp in cells lacking both Avpr1α and Oxtr.

We tested whether a specific Avpr2 inhibitor, tolvaptan, used in patients with chronic hyponatremia, affected bone formation and bone mass in wild-type and ovariectomized mice (20). Tolvaptan (20 mg·kg^{-1}·d^{-1}) was administered i.p. for 4 wk to mature 3-mo-old mice that were either sham-operated or ovariectomized. A week before they were killed, the mice were injected with calcein followed by xylenol orange for dynamic histomorphometry. Bone mineral density, measured by a PIXImus bone densitometer, declined at all sites upon ovariectomy (Fig. 3*A*). This decrement was neither reversed nor enhanced in tolvaptan-treated mice (Fig. 3*A*). Importantly, tolvaptan given to sham-operated mice did not reduce bone mass (Fig. 3*A*).

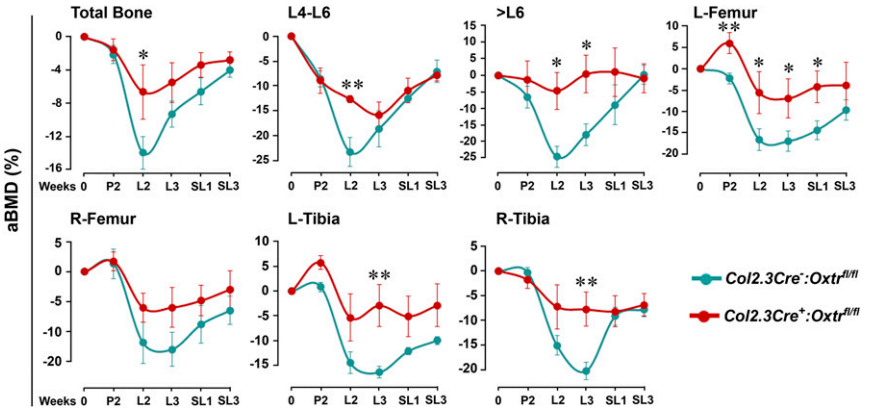

Fig. 4. Selective Oxtr deletion in osteoblasts attenuates lactation-induced bone loss, excluding an action of Oxt on the Avpr1α. Sequential areal BMD (aBMD) measurements (PIXImus, Lunar-GE), quantitated as changes (Δ) from prepregnancy BMD (0) in total bone, spine (L4–L6 and >L6), left and right femur (L- and R-Femur), and left and right tibia (L- and R-Tibia) at different time points during pregnancy week 2 (P2), lactation weeks 2 and 3 (L2 and L3) and weaning weeks 1 and 3 (SL1 and SL3) in *Col2.3Cre*$^{+}$*/Oxtr*$^{fl/fl}$ (n = 4) or *Col2.3Cre*$^{-}$*/Oxtr*$^{fl/fl}$ mice (n = 6 mice). Statistics: unpaired Student's t test; *$P \leq 0.05$, **$P \leq 0.01$.

Likewise, measurements of BV/TV in vertebral trabecular bone showed an expected reduction upon ovariectomy, with no reversal or accentuation with tolvaptan (Fig. 3*B*). Dynamic histomorphometry showed a decline in mineralizing surface and bone formation rate after ovariectomy which was unaffected by tolvaptan (Fig. 3*C*). The results show that specific inhibition of the Avpr2 does not affect bone mass in vivo.

We next studied whether Avpr1α or Avpr2 could be used by Oxt in a physiologic context when serum Oxt levels are high, such as during pregnancy or lactation. We therefore used lactating mice in which Oxtrs were specifically deleted in osteoblasts (10). Our hypothesis was that *Col2.3Cre*$^{-}$*:Oxtr*$^{fl/fl}$ mice would suffer greater lactation-induced bone loss because of the action of high Oxt levels on intact Avpr1αs. Bone mineral density (BMD) measurements revealed the expected loss of bone in both cortical and trabecular compartments in *Col2.3Cre*$^{-}$*:Oxtr*$^{fl/fl}$ mice, most profound at lactation weeks 2 and/or 3 (Fig. 4). However, this loss was markedly attenuated, rather than enhanced, in *Col2.3Cre*$^{+}$*:Oxtr*$^{fl/fl}$ mice lacking Oxtrs solely in osteoblasts (Fig. 4). This finding suggested that, in lactating mice, the actions of high circulating Oxt are not mediated through the Avpr1α or Avpr2. Otherwise, one would have seen even greater bone loss in *Col2.3Cre*$^{-}$*:Oxtr*$^{fl/fl}$ mice.

Discussion

Because Avp and Oxt are closely related nonapeptides that can act upon each other's receptors (14–17), we examined in depth the interaction of the two peptides at the receptor level in the physiologic context of bone mass regulation. *Avpr1α*$^{-/-}$ mice display a remarkable high bone mass phenotype, but double mutants lacking both receptors have only mildly increased bone mass, indicative of phenotypic rescue. Consistent with this phenotype, cells from *Oxtr*$^{-/-}$*:Avpr1α*$^{-/-}$ mice display a significant (albeit partial) reversal of Avp-induced reductions in osteoblast gene expression. Clinically, therefore, any skeletal effects of elevated AVP levels in patients with chronic hyponatremia, and particularly in patients with SIADH, will be exerted through both the AVPR1α and OXTR. However, the severe osteoporosis in patients with SIADH would indicate a dominant action of AVP, which is elevated up to 30-fold (21) through the AVPR1α.

AVP could indeed be a primary determinant for the osteoporosis that is known to accompany chronic hyponatremic states (22–28), although high aldosterone levels, for example in SIADH, may contribute also (21). The latter is possible because hyperaldosteronism also has been shown to cause bone loss in rodents (29, 30). Osteoporosis also is widely recognized as being associated with heart failure, particularly in elderly patients (31); the proposed pathophysiological mechanisms include secondary hyperparathyroidism, testosterone deficiency, and excessive inflammatory cytokine production (31–33). Nonetheless, inappropriate AVP secretion is also a hallmark of low-output cardiac failure and in these instances may contribute to bone loss. Our data also show that there is reciprocal regulation of Avp and Oxt secretion in mice—Oxt injections cause decrements in Avp, and vice versa (Fig. S1). Although to our knowledge the two hormones have never been measured in tandem in clinical situations, it is possible that low OXT levels may enhance the bone catabolic action of elevated AVP levels. Two translational paradigms thus arise from our studies: The first is the notion that AVP is a likely driver for bone loss in patients with chronic hyponatremia; the second is the imperative for measuring plasma OXT and AVP in cases where an association of osteoporosis, hyponatremia, and high AVP is suspected.

In contrast to Avpr1α, Avpr2 is localized primarily to the kidney, where it regulates water absorption. A selective, competitive AVPR2 inhibitor, tolvaptan, is currently in use to counteract the chronic hyponatremia of congestive cardiac failure, cirrhosis, and SIADH (20, 29). As noted above, although such conditions are associated with bone loss, now attributable in part to high AVP levels (21, 29), we show that, in wild-type and ovariectomized mice, tolvaptan neither offers osteoprotection nor adversely affects bone mass, in essence attesting to its selectivity for the kidney AVPR2.

Finally, to examine potential antianabolic actions of Oxt via the Avpr1α, we used a murine lactation model of bone loss in which the *Oxtr* was deleted specifically in osteoblasts (10, 34). Mice lose bone maximally at weeks 2 and 3 of lactation, after which there is prompt skeletal recovery at weaning. Several mechanisms, such as hypoestrogenemia and elevated Pthrp levels, have convincingly explained the intergenerational transfer of calcium from the maternal to fetal skeleton (35). However, the mechanism involved in skeletal recovery both in rodents and humans has remained unclear. Having found that bone formation is reduced in pregnant mice lacking the Oxtr, we speculated that high circulating Oxt levels might mediate the anabolic skeletal recovery (9). We thus hypothesized that the absence of the Oxtr selectively in osteoblasts will inhibit this physiologic anabolic response at weaning and in turn will worsen osteopenia, particularly because Oxt may act via the Avpr1α. However, osteoblast-selective *Oxtr* deletion in *Col2.3Cre*$^{+}$*:Oxtr*$^{fl/fl}$ mice prevented, rather than accentuated, lactation-induced bone loss. This reversal also excludes a putative action of high Oxt on an osteoclastic Avpr1α, which, according to our prior data (3),

should stimulate resorption. Instead, reduced circulating Avp levels in the face of high Oxt levels could explain reduced activation of the Avpr1α. Alternatively, high circulating Oxt levels could activate the osteoclast Oxtr to prevent the resorption of bone by mature osteoclasts (2).

Materials and Methods

All procedures were carried out with the approval by the IACUCs at Mount Sinai School of Medicine and the University of Bari. The generation of *Oxtr*$^{-/-}$, *Avpr1α*$^{-/-}$, and *Col2.3Cre*:*Oxtr*$^{fl/fl}$ mice has been reported (2, 3, 10). *Avpr1α*$^{-/-}$ mice were crossed with *Oxtr*$^{+/-}$ mice to generate double mutants. Ovariectomy was performed as described previously (10). Lactating mice were fed on normal chow ad libitum. Tolvaptan was provided by Otsuka America Pharmaceuticals. For histomorphometry, the mice were injected with xylenol orange (90 mg/kg, i.p.) and calcein (15 mg/kg, i.p.) 7 and 2 d before they were killed. Femurs were dissected, processed, and analyzed for bone formation parameters, as before (3). Bone marrow stromal cells were cultured in the presence of ascorbate-2-phosphate (1 mM) (Sigma) for mRNA and protein analysis. Alkaline phosphatase-positive cfu colonies were counted in 10-d cultures, and osteoblast gene expression was measured by qPCR (6). For the preparation of nucleoplasts, osteoblast-enriched cultures were obtained by sequential collagenase digestion of newborn calvaria. Intact nuclei were isolated as described by Adebanjo et al. (19). The outer nuclear membrane and nucleoplasts (nuclei without outer membranes) were separated. To detect Avpr1α expression, immunofluorescence was performed using a rabbit polyclonal anti-Avpr1α antibody and anti-rabbit Cy-3–conjugated secondary antibodies (Chemicon International Inc.) associated with 60 μg/mL fluorescein-labeled phalloidin (Sigma Aldrich). Mass spectrometric analysis of nuclear extracts is detailed in *SI Materials and Methods* (18). Western blotting was performed using rabbit polyclonal anti-Avpr1α, mouse monoclonal pErk, rabbit polyclonal total Erk (tErk) (Santa Cruz), and IRDye-labeled secondary antibodies (680/800CW) (LI-COR Biosciences). A LI-COR Odyssey infrared imaging system was used.

ACKNOWLEDGMENTS. This study was supported by NIH National Institute on Aging Grant AG40132 (to M.Z.), and by NIH Grants DK80459 (to M.Z. and L.S.) and AG23176, AR06592, and AR06066 (all to M.Z.). A.Z. is supported by the Italian Space Agency and the Italian Ministry of Education, Universities and Research.

1. Colaianni G, et al. (2014) The oxytocin-bone axis. *J Neuroendocrinol* 26(2):53–57.
2. Tamma R, et al. (2009) Oxytocin is an anabolic bone hormone. *Proc Natl Acad Sci USA* 106(17):7149–7154.
3. Tamma R, et al. (2013) Regulation of bone remodeling by vasopressin explains the bone loss in hyponatremia. *Proc Natl Acad Sci USA* 110(46):18644–18649.
4. Abe E, et al. (2003) TSH is a negative regulator of skeletal remodeling. *Cell* 115(2): 151–162.
5. Isales CM, Zaidi M, Blair HC (2010) ACTH is a novel regulator of bone mass. *Ann N Y Acad Sci* 1192:110–116.
6. Sun L, et al. (2006) FSH directly regulates bone mass. *Cell* 125(2):247–260.
7. Zaidi M (2007) Skeletal remodeling in health and disease. *Nat Med* 13(7):791–801.
8. Zaidi M, et al. (2010) ACTH protects against glucocorticoid-induced osteonecrosis of bone. *Proc Natl Acad Sci USA* 107(19):8782–8787.
9. Liu X, et al. (2009) Oxytocin deficiency impairs maternal skeletal remodeling. *Biochem Biophys Res Commun* 388(1):161–166.
10. Colaianni G, et al. (2012) Bone marrow oxytocin mediates the anabolic action of estrogen on the skeleton. *J Biol Chem* 287(34):29159–29167.
11. Nishimori K, et al. (1996) Oxytocin is required for nursing but is not essential for parturition or reproductive behavior. *Proc Natl Acad Sci USA* 93(21):11699–11704.
12. Birnbaumer M, et al. (1992) Molecular cloning of the receptor for human antidiuretic hormone. *Nature* 357(6376):333–335.
13. Sugimoto T, et al. (1994) Molecular cloning and functional expression of a cDNA encoding the human V1b vasopressin receptor. *J Biol Chem* 269(43):27088–27092.
14. Mouillac B, et al. (1995) The binding site of neuropeptide vasopressin V1a receptor. Evidence for a major localization within transmembrane regions. *J Biol Chem* 270(43): 25771–25777.
15. Chini B, et al. (1995) Tyr115 is the key residue for determining agonist selectivity in the V1a vasopressin receptor. *EMBO J* 14(10):2176–2182.
16. Wheatley M, et al. (2007) Extracellular loops and ligand binding to a subfamily of Family A G-protein-coupled receptors. *Biochem Soc Trans* 35(Pt 4):717–720.
17. Akerlund M, et al. (1999) Receptor binding of oxytocin and vasopressin antagonists and inhibitory effects on isolated myometrium from preterm and term pregnant women. *Br J Obstet Gynaecol* 106(10):1047–1053.
18. Di Benedetto A, et al. (2014) Osteoblast regulation via ligand-activated nuclear trafficking of the oxytocin receptor. *Proc Natl Acad Sci USA* 111(46):16502–16507.
19. Adebanjo OA, et al. (1999) A new function for CD38/ADP-ribosyl cyclase in nuclear Ca2+ homeostasis. *Nat Cell Biol* 1(7):409–414.
20. Dasta JF, et al. (2012) Update on tolvaptan for the treatment of hyponatremia. *Expert Rev Pharmacoecon Outcomes Res* 12(4):399–410.
21. Sejling AS, Pedersen-Bjergaard U, Eiken P (2012) Syndrome of inappropriate ADH secretion and severe osteoporosis. *J Clin Endocrinol Metab* 97(12):4306–4310.
22. Renneboog B, Musch W, Vandemergel X, Manto MU, Decaux G (2006) Mild chronic hyponatremia is associated with falls, unsteadiness, and attention deficits. *Am J Med* 119(1):71.e1–e8.
23. Kinsella S, Moran S, Sullivan MO, Molloy MG, Eustace JA (2010) Hyponatremia independent of osteoporosis is associated with fracture occurrence. *Clin J Am Soc Nephrol* 5(2):275–280.
24. Verbalis JG, et al. (2010) Hyponatremia-induced osteoporosis. *J Bone Miner Res* 25(3): 554–563.
25. Gankam Kengne F, Andres C, Sattar L, Melot C, Decaux G (2008) Mild hyponatremia and risk of fracture in the ambulatory elderly. *QJM* 101(7):583–588.
26. Sandhu HS, Gilles E, DeVita MV, Panagopoulos G, Michelis MF (2009) Hyponatremia associated with large-bone fracture in elderly patients. *Int Urol Nephrol* 41(3): 733–737.
27. Barsony J, Sugimura Y, Verbalis JG (2011) Osteoclast response to low extracellular sodium and the mechanism of hyponatremia-induced bone loss. *J Biol Chem* 286(12): 10864–10875.
28. Hoorn EJ, et al. (2011) Mild hyponatremia as a risk factor for fractures: The Rotterdam Study. *J Bone Miner Res* 26(8):1822–1828.
29. Balla T, Nagy K, Tarján E, Renczes G, Spät A (1981) Effect of reduced extracellular sodium concentration on the function of adrenal zona glomerulosa: Studies in conscious rats. *J Endocrinol* 89(3):411–416.
30. Chhokar VS, et al. (2004) Loss of bone minerals and strength in rats with aldosteronism. *Am J Physiol Heart Circ Physiol* 287(5):H2023–H2026.
31. Zotos P, et al. (2014) Bone metabolism in chronic heart failure. *J Osteopor Phys Act* 2(2):121.
32. Jankowska EA, et al. (2009) Bone mineral status and bone loss over time in men with chronic systolic heart failure and their clinical and hormonal determinants. *Eur J Heart Fail* 11(1):28–38.
33. Terrovitis J, et al. (2012) Bone mass loss in chronic heart failure is associated with secondary hyperparathyroidism and has prognostic significance. *Eur J Heart Fail* 14(3): 326–332.
34. Wysolmerski JJ (2002) The evolutionary origins of maternal calcium and bone metabolism during lactation. *J Mammary Gland Biol Neoplasia* 7(3):267–276.
35. VanHouten JN, Wysolmerski JJ (2003) Low estrogen and high parathyroid hormone-related peptide levels contribute to accelerated bone resorption and bone loss in lactating mice. *Endocrinology* 144(12):5521–5529.